CrossMark

ORIGINAL ARTICLE – CANCER RESEARCH

Lung carcinoma progression and survival versus amino- and carboxyl-parathyroid hormone-related protein expression

Randolph H. Hastings[1,2,4] · Philippe R. Montgrain[2,3,7] · Rick A. Quintana[2] ·
Boris Chobrutskiy[2] · Ashkhan Davani[2] · Atsushi Miyanohara[5] · Sepi Mahooti[6]

Abstract

Purpose Expression of the carboxyl PTHrP region of parathyroid hormone-related protein (PTHrP) is a positive prognostic indicator in women with lung cancer, but amino PTHrP is a negative indicator in other lung cancer patients. This project investigated whether PTHrP could be expressed as predominantly amino PTHrP or carboxyl PTHrP in individual lung carcinomas. It also assessed domain-specific effects on cancer progression and patient survival.

Methods PTHrP immunoreactivities were analyzed versus survival in a human lung cancer tissue microarray (TMA). Growth was compared in athymic mice for isogenic lung carcinoma xenografts differing in expression of amino and carboxyl PTHrP domains.

Results In the TMA, 33 of 99 patient tumors expressed only one PTHrP domain, while 54 expressed both. By Cox regression, the hazard ratio for cancer-specific mortality (95% confidence interval) was 2.6 (1.28–5.44) for amino PTHrP ($P = 0.008$) and 0.6 (0–2.58) for carboxyl PTHrP ($P = 0.092$). Xenografts of H358 lung adenocarcinoma cells that overexpressed amino PTHrP grew twice as fast as isogenic low PTHrP tumors in athymic mice, but growth of tumors expressing amino plus carboxyl PTHrP was not significantly different than growth of the control tumors. In summary, the presence of amino PTHrP signifies worse prognosis in lung cancer patients. In mouse xenografts, this effect was abrogated if carboxyl PTHrP was also present.

Conclusion Amino PTHrP and carboxyl PTHrP can vary independently in different lung carcinomas. Carboxyl PTHrP may temper the stimulatory effect of amino PTHrP on cancer progression.

Keywords Neuroendocrine and other endocrine factors · Molecular diagnosis and prognosis · Biochemical markers · Carcinoma, non-small cell lung · Oncogenes · Tumor suppressor proteins

✉ Randolph H. Hastings
  rhhastings@ucsd.edu

1 Anesthesiology Service, VA Medical Center (125), VA
   San Diego Healthcare System, 3350 La Jolla Village Dr.,
   San Diego, CA 92161, USA

2 Research Service, VA San Diego Healthcare System,
   San Diego, USA

3 Medicine Service, VA San Diego Healthcare System,
   San Diego, USA

4 Department of Anesthesiology, UC San Diego, San Diego,
   USA

5 Viral Vector Core, UC San Diego, San Diego, USA

6 Pathology Service, VA San Diego Healthcare System,
   San Diego, USA

7 Department of Medicine, UC San Diego, San Diego, USA

Introduction

Parathyroid hormone-related protein (PTHrP) has prominent roles in cancer pathology, fetal development, and the function of many normal tissues. PTHrP can have an impact on several factors related to cancer progression, such as apoptosis, tumor growth, and angiogenesis (Akino et al. 2000; Bakre et al. 2002; Chen et al. 2002; Isowa et al. 2010; Luparello et al. 1997). The protein's action can be stimulatory or inhibitory in different situations. Diversity and variability in PTHrP effects is not surprising because it is a multifunctional pro-hormone

with biologically active amino-terminal, carboxyl PTHrP-terminal, and mid-molecule domains (Orloff et al. 1996; Philbrick et al. 1996). Furthermore, the primary structure of PTHrP includes multiple single- and multi-basic cleavage sites. Post-translational processing depends on context and can produce a diverse collection of daughter peptides that can vary among tissues and even among tumors with the same histology (Orloff et al. 1994).

In lung cancer, PTHrP is conceptually linked with hypercalcemia of malignancy, but effects on cancer progression have also been recognized. We published two studies with different groups of patients that suggested that carboxyl PTHrP was a positive prognostic indicator for women with non-small cell lung cancer (NSCLC) (Hastings et al. 2006; Montgrain et al. 2011). Interestingly, a study from another research group proposed that amino PTHrP was associated with shorter overall survival times in patients of both sexes with NSCLC (Monego et al. 2009), contrary to the finding for carboxyl PTHrP. One would not expect amino PTHrP and carboxyl PTHrP to demonstrate opposing effects on survival if their expression was always linked. Thus, the seemingly conflicting results from the different studies could mean that PTHrP processing varies among individual lung cancers (Hook et al. 2001; Orloff et al. 1994), with some lung carcinomas expressing only the amino domain and others restricted to the carboxyl PTHrP domain. Literature reports for human lung carcinoma place prevalence at 50–85% for amino PTHrP immunoreactivity and 65–85% for carboxyl PTHrP (Asa et al. 1990; Hastings et al. 2006; Kitazawa et al. 1991; Monego et al. 2009) but data on joint expression of the two regions are not available.

In summary, the current state of the literature suggests that PTHrP may have a variable action as either a positive or a negative prognostic indicator in lung cancer and that variation in expression of amino PTHrP versus carboxyl PTHrP could impact the hormone's relationship with lung cancer progression and patient survival. However, there are no studies that have compared amino PTHrP and carboxyl PTHrP head-to-head in the same group of lung carcinomas. Also, no survival studies have investigated how the two domains together or separately affect tumor behavior and patient survival. Thus, the goals of this project were to compare expression of amino PTHrP against expression of carboxyl PTHrP in individual lung carcinomas, to evaluate how survival of lung cancer patients varied with regard to expression of both PTHrP regions, and to manipulate amino PTHrP and carboxyl PTHrP expression in a mouse model of lung cancer to compare effects on cancer cell proliferation, tumor growth, and angiogenesis.

Materials and methods

Experimental plan

An observational study was planned to compare the expression of amino and carboxyl PTHrP domains in human lung cancer tissue microarrays and to evaluate what impact those moieties had on patient survival. Two tissue microarrays (TMA) from IMGENEX (IMH-305 and IMH-358, San Diego, CA) were used because they provided tissue from 98 patients with non-small cell lung carcinoma along with the necessary demographic information and survival data. The arrays were accompanied with the data necessary for most of the independent variables, including age, gender, cancer stage, tumor histology, tumor size, and lymph node involvement. We assessed amino PTHrP and carboxyl PTHrP immunoreactivities as additional independent variables. Dependent variables were disease-specific mortality and overall mortality, information that was also provided with the TMA.

To gain further insight about lung cancer PTHrP expression and effects, we evaluated archived lung carcinoma surgical specimens from the UC San Diego Department of Pathology. This study was a post hoc examination of samples that had been previously evaluated for carboxyl PTHrP (Hastings et al. 2006). Specimens came from patients who had undergone surgery at UC San Diego Medical Center for NSCLC resection between 1987 and 1996. Archived lung cancer tissue was available for 207 patients out of the original group of 221 who were analyzed in the previous study (Hastings et al. 2006). The same independent variables were used as in the tissue microarray study. Amino PTHrP immunohistochemical staining was performed for the post hoc study. Carboxyl PTHrP staining results were provided by the previous research effort. The only dependent variable was overall survival because disease-specific data were not available for this group. Patient survival was updated for 18 patients who had continued follow-up past publication of the 2006 study. The studies were approved by the UC San Diego and VA San Diego Healthcare System Institutional Review Boards. The boards' requirement for informed consent was waived based on institutional criteria.

A direct comparison of the effects of amino PTHrP and carboxyl PTHrP on the characteristics of lung carcinoma growth was conducted with xenograft experiments in immunocompromised mice. Xenografts were formed with human NCI-H358 lung adenocarcinoma cells, a line derived from an adenocarcinoma in situ (McLemore et al. 1987), i.e., a bronchoalveolar carcinoma. Our assays reveal that the wild-type H358 cells express only low levels of PTHrP protein. The experimental manipulation was overexpression of various PTHrP domains

introduced by transducing the cells with lentiviral vector containing either no PTHrP insert, full-length PTHrP 1–139, PTHrP 1–87, or PTHrP 33–139. The result was stable, isogenic clones that expressed either low levels of both PTHrP domains, high levels of PTHrP with both amino- and carboxyl PTHrP present, high levels of amino PTHrP alone, or high levels of carboxyl PTHrP alone. Outcomes were established before beginning experiments. These measures were caliper estimates of tumor volume versus time after tumor implantation, mouse weight versus time, microscopic mitotic figure density of tumor at completion of the experimental period, and microscopic tumor CD31 staining indices. Tumors were followed for 5 weeks after implantation, shortly less than the time for tumors to reach the maximum size allowed by the local institutional animal care and use committee (IACUC). Animal experiments were approved by the IACUC. The study followed the United States Public Health Service Policy on Human Care and Use of Laboratory Animals and adhered to policies set forth in the Guide for the Care and Use of Laboratory Animals.

PTHrP immunohistochemistry

The human lung cancer TMA displayed formalin-fixed lung carcinoma surgical samples, each represented as a 2 mm core sectioned at a thickness of 4 μM. The manufacturer supplied one slide for each array already stained with hematoxylin and eosin.

Amino PTHrP was probed with rabbit polyclonal antibody T4512 (Bachem, Inc., Torrance, CA, USA). Separate slides were stained for carboxyl PTHrP with antibody 9H7 directed against an epitope within residues 119–127 of PTHrP. The two antibodies were the same as those used in the previous amino PTHrP and carboxyl PTHrP studies (Hastings et al. 2006; Monego et al. 2009). Sections were incubated with primary antibody for 1 h at room temperature. Staining was produced with a standard ABC alkaline phosphatase method using the Vector Red kit from Vector Laboratories (SK-5100, Burlingame, CA, USA). Sections were counterstained with methyl green, as described previously (Hastings et al. 2006). Optimal antibody dilution was established by testing T4512 and 9H7 over the range of 10–20 μg IgG/ml on pilot TMA slides and larger lung carcinoma sections from known PTHrP-positive tumors. Concentrations were selected that generated well-defined intracellular reaction product with limited background. For negative controls, the primary antibody was omitted or preadsorbed with a 100-fold excess of PTHrP. Interassay controls were known PTHrP-positive lung carcinomas.

Slide evaluation

A practicing surgical pathologist (SM) examined the Imgenex TMA in a blinded fashion. He assessed tissue preservation, staining quality, and PTHrP immunoreactivity. Quality control points included intracellular localization of immunoreactivity, minimal non-cellular debris, and absence of high background staining except at tissue edges. Uneven staining, excessive debris, and loss of adhesion to the slide were considerations to repeat staining on additional slides. Necrotic areas were avoided when evaluating immunoreactivity.

TMA immunoreactivity was quantitated by H-score. The H-score is based on two parts, an evaluation of intensity on a 0 to 3+ scale and an estimation of the percentage of cells staining at each intensity level (Hirsch et al. 2003; Lee et al. 2010). The H-score is calculated as the sum of the products of intensity score times staining percentage. Thus, the score can range from 0 to 300.

Amino PTHrP staining of the archived UC San Diego surgical specimens was graded on a binary scale based on the presence or absence of immunoreactivity in excess of background levels. This metric was used to match the assessment performed for carboxyl PTHrP in the previous investigation. The carboxyl PTHrP staining in the previously stained specimens had faded with time, which precluded updating the PTHrP assessment to H-scores.

Cell culture

The NCI-H358 cell line (ATCC, Manassas, VA) has been authenticated by ongoing examination of morphology, assessment of growth rate, and measurement of PTHrP. Cells were grown in RPMI-1640 plus 10% fetal bovine serum at 37 °C in a humidified atmosphere of 5% carbon dioxide, 95% air. All cell lines were tested for mycoplasma infection using the MycoAlert kit (Lonza, Basel, Switzerland) within the last year and verified free of infection. Viability measured with Trypan blue staining prior to manipulations and experiments was >98%.

PTHrP lentiviral vectors

Mammalian expression plasmids for human prepro PTHrP 1–87 in the pCMV5 vector (Addgene), PTHrP 1–139, and PTHrP 33–139 had been generated previously (Tsigelny et al. 2005) in the pci-Neo vector (Promega). After verifying identity and integrity by sequencing, the PTHrP 1–87 insert was excised with restriction enzymes BglII and Sma1, then recloned into the BamH1 and Pme1 sites downstream of the CMV promoter in the HIV1 vector plasmid pHIV1-CMV-RSV-Neo (Yam et al. 2002). Similarly, the PTHrP 1–139 and PTHrP 33–139 sequences were isolated

by NheI and NotI digestion and inserted distal to the CMV promoter in the same vector. Lentiviral vectors were grown by transient transfection of 293T cells. Cells in 150 mm dishes were co-transfected by polyethyleneimine method with each HIV1 vector plasmid, pLP1 and pLP2 (Invitrogen), and pCMV-G (Yee et al. 1994). Conditioned media were collected at day 1, 2, and 3 post-transfection, filtered through a 0.45 μM filter, and concentrated by centrifugation in a Sorvall GS-3 rotor at 7000 rpm for 16 h at 4 °C. The resulting pellets were suspended in 10 mM Tris HCl buffer, pH 7.8, containing 1 mM MgCl$_2$, and 3% sucrose. Vectors were produced by Dr. Atsushi Miyanohara of the UC San Diego Vector Laboratory.

H358 lung cancer cells that had been maintained for no more than 5 passages since purchase were transfected with each of the three lentiviral PTHrP vectors or with empty vector. Exponentially growing cells at 70% confluency were incubated with 4 μg/ml hexadimethrine bromide plus lentivirus at a concentration of 2×10^5 infectious units/1×10^6 cells in fresh media for 18 h at 37 °C and then replenished with fresh media. Transfection efficiency with a lentiviral EGFP clone was 75%. Transfected clones were selected with G418 and expanded. PTHrP expression was verified by immunoassay. Cells followed for 4 weeks in culture produced constant levels of the ectopic PTHrP over that period.

PTHrP immunoassay

Conditioned media and cell extracts were assayed by region-specific immunoassays for PTHrP (Deftos 2001; Montgrain et al. 2007). Amino PTHrP was measured with a two site fluorescent assay using a monoclonal antibody 1A5 against PTHrP 15–34 for capture, a rabbit polyclonal antibody recognizing PTHrP 1–5 for detection, and human PTHrP 1–34 as standard. The assay has a broad linear range from 8 to 5000 pg/ml, in molar terms roughly 10^{-12} to 10^{-9} M. Carboxyl PTHrP was measured by radioimmunoassay using a rabbit polyclonal antibody raised against PTHrP 129–139 peptide in a three-day non-equilibrium format, as described previously (Montgrain et al. 2007). The tracer, tyr-PTHrP 109–138, was radioiodinated with the chloramine-t method, and the standard curve was constructed with unlabeled human PTHrP 109–141. The minimum level of detection is 1–7 pmol/L, while the intra- and interassay variations are approximately 7–12%. The assays have been validated by measurements of various PTHrP standards (epitope size peptides up to full-length proteins, peptides lacking, or including the target sequence) and related non-PTHrP proteins (calcitonin, PTH, and chromogranin). The assays do not cross-react with other proteins. Furthermore, the assays accurately track changes in PTHrP concentration caused by adding known quantities of exogenous peptide to lung cancer cell lysates or tissue homogenates (Brandt et al. 1991; Deftos et al. 1993). Samples were assayed in triplicate in multiple dilutions that paralleled the corresponding standard curve.

Cell proliferation assay

H358 cells were plated in 96-well plates at a density sufficient to result in 1500 adherent cells/well after 18 h in culture. The media was replenished at that point and cells were allowed to proliferate for 0, 2, 4, or 6 days. Cell number was assayed at these time points based on 1 h uptake of 3-(4,5-dimethylthiazol-2-yl)-5-(3-carboxymethoxyphenyl)-2-(4-sulfophenyl)-2H-tetrazolium (MTS), as previously described (Montgrain et al. 2015). Absorbance of bioreduced compound was read at 490 nm. Standard curves relating signal to cell number were constructed for each cell line and time point. Results are reported based on cell number.

Mouse xenograft model

Human lung cancer cells were harvested from subconfluent cultures by brief trypsinization, washed in medium and phosphate-buffered saline, and then suspended in serum-free iced medium with 250 μg/mL Matrigel at a density of 2×10^4 cells/μL. Viability was >95% by Trypan blue staining. Cells were kept on ice until flank implantation. Female athymic mice at 5 weeks of age were lightly anesthetized, and 1×10^6 cells in 50 μl were injected subcutaneously in one flank through a 25-gauge needle. Female mice were selected to be able to detect the action of carboxyl PTHrP in the event that female gender was necessary to observe the effect (Hastings et al. 2006; Montgrain et al. 2011). Mice were weighed weekly and tumor width and lengths were measured with calipers under light anesthesia. Animals were euthanized at 5 weeks after implantation, close to the period at which the area of control tumors reaches 1 cm^2, the institutional limit. At that time, tumors were measured, dissected from the flank, fixed in 2% buffered paraformaldehyde, and embedded in paraffin for assessment of proliferation and angiogenesis markers. Animal studies were approved by the local institutional animal care and use committee.

Mouse tissue processing and analysis

Tumor sections were cut at a thickness of 5 μM, mounted on glass slides, and deparaffinized through a graded ethanol series. Histologic and morphologic characteristics were assessed on slides stained with Harris hematoxylin and eosin Y. These slides were examined for mitotic bodies as a measure of tumor cell proliferation. Briefly, slide identity

was masked and an evaluator counted and summed mitotic bodies in 50 adjacent fields across the tumor at 40x magnification. At this magnification, all 50 fields were filled with tumor. Additional slides were stained by immunohistologic methods for CD31, a vascular endothelial marker to assess tumor angiogenesis. Antigen retrieval was performed by soaking slides overnight in a 60 °C Tris–EDTA-1%Tween20 bath adjusted to 9.0 pH. CD31 staining used rabbit polyclonal antibody ab28364 (abcam, Cambridge, MA, USA) diluted 1/50 and a goat anti-rabbit IgG H&L Alexa Fluor 488 secondary antibody (abcam ab150081) diluted 1/200. CD31 was evaluated on 30-adjacent 40× magnification images of each slide. A binary threshold was adjusted to highlight the fluorescent region and the area of CD31 staining was measured with ImageJ (NIH).

Data analysis

Categorical data were tabulated as frequencies and percentages, and continuous variables were reported as medians. Relationships between categorical variables were analyzed with the chi-squared test with the Yates continuity correction, while continuous data were compared among groups by Wilcoxon rank test, Mann–Whitney U score, or Kruskal–Wallis test. The impact of amino PTHrP and carboxyl PTHrP H-score and other covariates on survival was performed with Cox proportional hazards regression (StatView 5.0.1, SAS Institute, Cary, NC, USA) (R Development Core Team 2004). Proliferation of cultured cells, growth of tumor xenografts, xenograft mitotic body density, xenograft CD31 staining index, and weight of tumor-bearing mice were compared as a function of expression of amino and carboxyl PTHrP domains, alone or expressed together, by analysis of variance (Prism, Graph-Pad Software, San Diego, CA, USA). The level for statistical significance was 0.05.

Results

Amino and carboxyl PTHrP expression in human lung carcinomas TMA

Median H-scores (interquartile gap) were 120 (40–180) for amino PTHrP and 140 (33–200) for carboxyl PTHrP ($P < 0.13$). Histograms of H-scores showed that the most common result was a score of 0 in sections stained for amino PTHrP and also in those stained for carboxyl PTHrP. A broad distribution of tumors had scores for either epitope above 50 (Fig. 1a). The histograms demonstrate a valley separating the tumor sections into populations with scores of 50 or less and those scoring greater than 50. Thus, a 50 score was selected as the cut-off for each epitope to separate specimens into those with high and low immunoreactive staining. When individual tumor amino PTHrP immunoreactivity was compared to the corresponding carboxyl PTHrP staining, discordance in scores was found in 32 patients, a third of the population. Tumors had high H-scores only for amino PTHrP in 15 patients, and high carboxyl PTHrP staining alone

Fig. 1 Histograms of H-scores for PTHrP immunoreactivity in TMA lung cancer specimens. The upper panels show univariate histograms for amino PTHrP staining on the *left* and carboxyl PTHrP on the *right*. Both histograms include a preponderance of tumors scoring 0 and broad distribution of tumors with scores above 50. Thus, low staining was defined as a score of 50 or below for each PTHrP epitope. The bottom graph shows amino PTHrP and carboxyl PTHrP staining for patients divided on the basis of high and low tumor staining for each epitope. The largest group had significant staining for both domains, but tumors in some patients were restricted to amino PTHrP or carboxyl PTHrP immunoreactivity alone
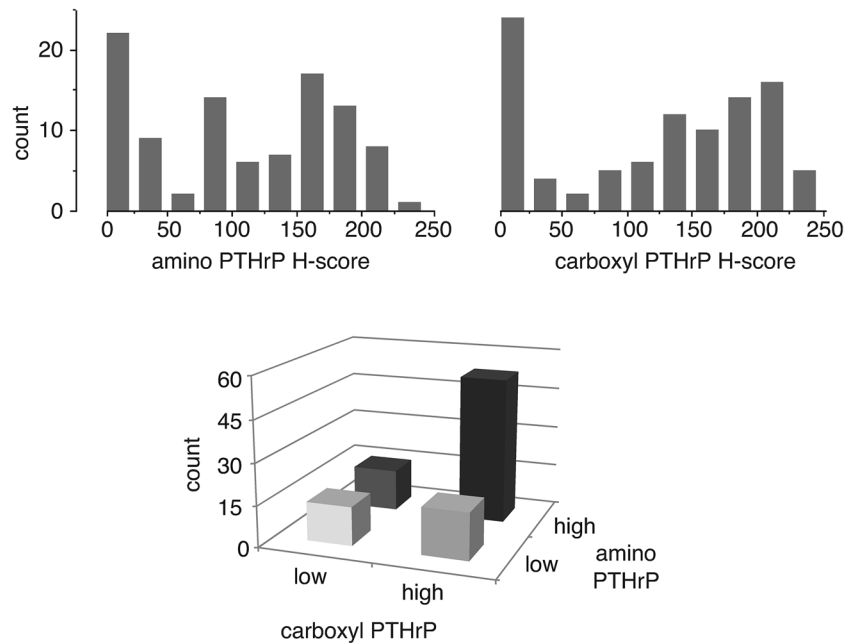
in 17 patients. Amino and carboxyl PTHrP were more likely to be expressed together than separately. In all, 53 patients had high H-scores for both epitopes and 14 had both scores low (Fig. 1b), significantly greater numbers than expected if amino PTHrP immunoreactivity and carboxyl PTHrP immunoreactivity were truly independent (X^2 4.44, $P = 0.031$).

Demographics, cancer data, and tumor PTHrP expression

Over three-quarters of the patients represented in the TMA were male (Table 1). Age ranged from 26 to 81 years and averaged 58 ± 1 years. Lung cancer histology was squamous cell carcinoma in half the patients, adenocarcinoma in 36%, and large cell or poorly differentiated histology in the remainder. The majority of patients had stage 1 or 2 disease. Tumor diameter was less than or equal to 3 cm in over 80% of the patients and 42% had nodal involvement, N1 in 23 patients and N2 in 19. Amino PTHrP and carboxyl PTHrP H-scores did not vary based on sex, age, histology, stage, tumor size, or nodal involvement.

Survival analyses

Median follow-up time was 43 months with a range of 2–149 months. During the evaluation period, 49 patients died as a result of their lung cancer and 57 patients died in total, representing cancer-specific mortality and overall mortality, respectively. High amino PTHrP staining was associated with a univariate hazard ratio of 1.70 (0.93–3.10, 95% confidence limits) for overall mortality ($P = 0.087$) and 2.24 (1.12–4.48) for cancer-specific mortality ($P = 0.022$) (Table 2). In the multivariate Cox analysis, the hazard ratio for high amino PTHrP staining was also significantly greater than 1 for both overall mortality and cancer-specific mortality. The hazard ratios for high carboxyl PTHrP staining were less than 1 but not significantly different from unity for any of the analyses. Stage was also a significant predictor of mortality, but age, gender, and histology were not. Hazard ratios for overall mortality were 1.87 (0.99–3.53) and 2.59 (1.28–5.26) for stage 2 and stage 3, respectively, and for cancer-specific mortality, the ratios were 1.88 (0.95–3.70) and 2.93 (1.38–6.20), respectively. Since stage, tumor size, and nodal involvement correlated with each other, stage was the only variable out of these three included in the multivariate analysis.

Table 1 Patient demographics versus amino PTHrP and carboxyl PTHrP expression for tissue microarrays

Factor	aPTHrP $H < 50$	aPTHrP $H > 50$	χ^2	P value	Effect size	cPTHrP $H < 50$	cPTHrP $H > 50$	χ^2	P value	Effect size
Total no.	31 (31.3)	68 (68.7)				29 (29.3)	70 (70.7)			
Gender										
Female	6 (28.6)	15 (71.4)	0.002	0.966	0.031	9 (42.9)	12 (57.1)	1.616	0.176	0.155
Male	25 (32.1)	53 (67.9)				20 (25.6)	58 (74.4)			
Age										
<60 years	16 (34.8)	30 (65.2)	0.229	0.521	0.070	15 (32.6)	31 (67.4)	0.208	0.516	0.068
≥60 years	15 (28.3)	38 (71.7)				14 (26.4)	39 (73.6)			
Histology										
Adeno	15 (42.9)	20 (57.1)	3.383	0.184	0.182	7 (20.0)	28 (80.0)	2.194	0.334	0.147
Squamous	13 (25.5)	38 (74.5)				16 (31.4)	35 (68.6)			
Large cell	3 (23.1)	10 (76.69)				2 (15.4)	11 (84.6)			
Stage										
1	10 (26.3)	28 (73.7)	1.096	0.578	0.105	10 (26.3)	28 (73.7)	1.096	0.578	0.105
2	12 (31.6)	26 (68.4)				12 (31.6)	26 (68.4)			
≥3	9 (39.1)	14 (60.9)				9 (39.1)	14 (60.9)			
Tumor size										
≤3 cm	24 (29.6)	57 (70.4)	0.238	0.575	0.077	22 (27.2)	59 (72.8)	0.498	0.392	0.099
>3 cm	7 (38.9)	11 (61.1)				7 (38.9)	11 (61.1)			
Lymph node involvement										
No	15 (26.3)	42 (73.7)	0.302	0.274	0.126	14 (24.6)	43 (75.4)	0.968	0.267	0.121
Yes	16 (38.1)	26 (61.9)				15 (35.7)	27 (64.3)			

Data are cell number (percentage for row)

aPTHrP amino PTHrP, *cPTHrP* carboxyl PTHrP, *H* H-score

Table 2 Relationship between PTHrP immunoreactivity and mortality of patients represented in the NSCLC tissue microarray

Factor	Overall survival				Cancer-specific survival			
	Univariate analysis		Multivariate analysis		Univariate analysis		Multivariate analysis	
	Hazard ratio (95% confidence limits)	P value	Hazard ratio (95% confidence limits)	P value	Hazard ratio (95% confidence limits)	P value	Hazard ratio (95% confidence limits)	P value
aPTHrP								
Low	Reference							
High	1.70 (0.93–3.10)	0.087	2.01 (1.07–3.78)	0.031	2.24 (1.12–4.48)	0.022	2.64 (1.28–5.44)	0.008
cPTHrP								
Low	Reference							
High	0.71 (0.41–1.23)	0.224	0.58 (0.33–1.02)	0.061	0.78 (0.16–3.91)	0.412	0.59 (0.00-258.0)	0.092

The TMA survival analysis was repeated counting any PTHrP immunoreactivity above background as a positive result for either epitope, rather than using an H-score of 50 as the cutpoint. The purpose was to match the scoring framework that was used for UC San Diego lung carcinoma specimens (see "Follow-up investigation on previously studied UC San Diego lung carcinoma specimens"), since it was not possible to evaluate H-scores on those samples. With these parameters, sections from 77 out of the 99 patients were amino PTHrP-positive and 74 were carboxyl PTHrP-positive. Cox regression found that amino PTHrP expression then carried significantly increased odds of cancer-specific death, 2.17 (1.00–4.73). Carboxyl PTHrP was associated with a lower hazard ratio, 0.57 (0.31–1.03), that did not cross the threshold for significance ($P = 0.061$).

Follow-up investigation on previously studied UC San Diego lung carcinoma specimens

Additional information regarding the relationships among amino PTHrP, carboxyl PTHrP and survival was sought with the post hoc investigation of lung carcinoma specimens available from our 2006 study of carboxyl PTHrP and lung cancer survival. The population of 207 patients included 119 males and 88 females (Table 3). The patients averaged 63.6 ± 0.8 years of age with 29% being less than 60 years old. Adenocarcinomas made up 40% of the histologies, 53% were squamous carcinoma and large cell carcinoma the balance. The majority of the patients had stage 1 or 2 disease, tumors ≤3 cm in diameter, and no lymph node involvement. The tumor immunoreactivity for amino PTHrP did not vary with any of the demographic or cancer-related factors. Carboxyl PTHrP immunoreactivity was more common for UC San Diego patients with higher stage tumors ($P = 0.038$), but did not vary with other demographic or cancer factors. Combined expression of amino PTHrP and carboxyl PTHrP in the same tumor was found in 62 patients, significantly higher than expected if the two epitopes were independent of each other ($P = 0.009$).

Amino PTHrP-positive/carboxyl PTHrP-negative tumors occurred in 16 patients and isolated expression of carboxyl PTHrP was found in 80 patients. Thus, discordant expression of the two epitopes existed in 46% of this group of patients.

In univariate analyses, the hazard ratio for overall mortality was 1.16 (0.90–1.49) for amino PTHrP (not significant at $P = 0.24$) and 0.70 (0.51–0.97) for carboxyl PTHrP ($P = 0.016$) (Table 4). Cancer-specific mortality was not available for this group. When the two epitopes were combined in a multivariate analysis, the amino PTHrP hazard ratio increased to 1.32 and approached the threshold for significance at $P = 0.051$. The carboxyl PTHrP hazard ratio was 0.65 (0.49–0.87) ($P = 0.003$). Histology and stage were also significant predictors of mortality. With squamous carcinoma as reference, the univariate and multivariate hazard ratios for adenocarcinoma were 0.62 (0.48–0.82) ($P < 0.001$) and 0.59 (0.43–0.82) ($P = 0.002$), respectively. With stage 1 as reference, the multivariate hazard ratios for stage 2 and stage 3 were 2.11 (1.11–3.80) ($P = 0.013$) and 3.24 (2.30–4.58) ($P < 0.0001$), respectively. Age and gender did not have a significant association with survival in the UC San Diego patients.

PTHrP expression by lentiviral-transduced H358 cell clones

Wild-type H358 cells produced 1.7 ± 0.2 pg amino PTHrP/μg cell protein and 0.8 ± 0.1 pg carboxyl PTHrP/μg cell protein in a 24-h period, expression levels on the lower end for human lung cancer cell lines (Table 5). Figure 2 demonstrates the augmented expression of PTHP by H358 cells after lentiviral transduction. Cells transfected with empty vector lacking PTHrP sequences contained low levels of intracellular PTHrP and secreted minimal quantities of the protein. Transduction with the PTHrP 1–87 vector and with the PTHrP 1–139 vector increased 24-h secretion of amino PTHrP to approximately 15 pg/μg cell protein. Transduction with the PTHrP 1–139 and with the PTHrP 33–139

Table 3 Demographics versus amino PTHrP and carboxyl PTHrP expression for UC San Diego patients with NSCLC

Factor	aPTHrP negative	aPTHrP positive	χ^2	P value	effect size	cPTHrP negative	cPTHrP positive	χ^2	P value	Effect size
All patients	129 (62.3)	78 (37.7)				65 (31.4)	142 (68.6)			
Gender										
Female	54 (61.4)	34 (38.6)	0.01	0.921	0.017	26 (29.5)	62 (70.5)	0.118	0.652	0.034
Male	75 (63.0)	44 (37.1)				39 (32.80)	80 (67.2)			
Age										
<60 years	42 (60.9)	27 (39.1)	0.023	0.763	0.021	16 (23.2)	53 (76.8)	2.697	0.082	0.125
≥60 years	87 (63.0)	51 (37.0)				49 (35.5)	89 (64.5)			
Histology										
Adeno	53 (63.9)	30 (36.1)	0.151	0.927	0.027	23 (27.7)	60 (72.3)	2.173	0.337	0.102
Squamous	67 (61.5)	42 (38.5)				35 (32.1)	74 (67.9)			
Large	9 (60.0)	6 (60.0)				7 (46.7)	8 (53.3)			
Stage										
1	77 (63.1)	45 (36.9)	3.593	0.166	0.131	30 (24.6)	92 (75.4)	6.522	0.038	0.175
2	10 (62.5)	6 (37.5)				6 (37.5)	10 (62.5)			
≥3	34 (49.3)	35 (50.7)				29 (42.0)	40 (58.0)			
Tumor										
≤3 cm	80 (67.2)	39 (32.8)	0.235	0.545	0.049	35 (29.4)	84 (70.6)	0.003	0.82	0.023
<3 cm	16 (57.1)	12 (42.9)				9 (32.1)	19 (67.9)			
Lymph nodes										
Involved	28 (62.2)	17 (37.8)	0	0.854	0.017	13 (28.9)	32 (71.1)	0	0.999	0.001
Not involved	64 (64.0)	36 (36.0)				29 (29.0)	71 (71.0)			
cPTHrP positive	80 (56.3)	62 (43.7)	6.105	0.009	0.182	0 (0.0)	142 (100.0)			
cPTHrP negative	49 (75.4)	16 (24.6)				65 (100.0)	0 (0.0)			

Data are cell number (percentage for row)

Negative signifies that tumor staining was no different than control

Positive signifies the presence of tumor immunoreactivity for the PTHrP epitope

aPTHrP amino PTHrP, *cPTHrP* carboxyl PTHrP

Table 4 Relationship between PTHrP immunoreactivity and mortality of UC San Diego patients with NSCLC

Factor	Univariate analysis		Multivariate analysis	
	Hazard ratio (95% confidence limits)	P value	Hazard ratio (95% confidence limits)	P value
aPTHrP				
Low	Reference			
High	1.16 (0.90–1.49)	0.241	1.32 (1.00-1.70)	0.051
cPTHrP				
Low	Reference			
High	0.71 (0.55–0.93)	0.014	0.65 (0.49–0.87)	0.003

Table 5 Amino PTHrP and carboxyl PTHrP expression in lung cancer cell lines (mean ± SE, $n = 3$ per line)

Line	Histology	Amino PTHrP, pg/μg	Carboxyl PTHrP, pg/μg
H358	Adeno	1.7 ± 0.2	0.8 ± 0.1
H1781	Adeno	6.7 ± 0.8	2.0 ± 0.2
H226	Squamous	3.6 ± 0.4	1.6 ± 0.1
H520	Squamous	6.6 ± 0.4	1.8 ± 0.1
H650	Large cell	2.8 ± 0.4	3.9 ± 0.1
H727	Carcinoid	3.3 ± 0.2	4.4 ± 0.1

PTHrP values are the sum of the quantity in 24-h conditioned media plus the content of the lysed cell layer

Data are normalized to the protein content of the underlying cell layer

vector increased carboxyl PTHrP secretion to 45–50 pg/μg cell protein. Transduction with PTHrP 1–87 vector did not stimulate carboxyl PTHrP, and the PTHrP 33–139 vector had no effect on amino PTHrP expression, as expected.

Effect of PTHrP domains on H358

Lentiviral-mediated overexpression of any of the PTHrP forms, PTHrP 1–87, PTHrP 33–139, and PTHrP 1–139, caused H358 cells to grow slower than isogenic cells transduced with lentiviral particles without a PTHrP insert. Cell numbers for the vector group were significantly greater by a factor of 1.33 than numbers in each of the other groups at day 4 and day 6 ($P < 0.0001$).

H358 cell xenograft results

Implantation of H358 cells generated tumors that could be detected by gross observation and microscopic examination in 33 of the 35 mice. No tumors could be found over the course of 5 weeks in 2 mice injected with cells from the PTHrP 1–139 clone. The growth of tumors in individual mice is plotted versus time after implantation and shown in the top panel in Fig. 3. At week 5 after implantation, the largest tumors were found in animals in the PTHrP 1–87 group. The lower panel in Fig. 3 shows the results of two-way ANOVA for time and PTHrP isoform on the left and a composite graph on the right showing the average estimated tumor volume for each group plotted versus time. Tumor volume increased significantly with time and also demonstrated a significant interaction between time and PTHrP isoform. In the graph in the lower panel, tumors in the PTHrP 1–87 group were significantly larger, 50–100% bigger on average, than tumors in the vector control group at weeks 4 and 5. The other two groups, PTHrP 33–139 and PTHrP 1–139, did not display significant differences compared with any group. Bars are not shown for the PTHrP 1–139 group at weeks 4 and 5 because three animals with the largest tumors

Fig. 2 Amino PTHrP and carboxyl PTHrP expression in H358 cell lines transduced with lentiviral vectors. Conditioned media and underlying cell layer were harvested after 24 h in culture to assay PTHrP secreted into the media or remaining inside the cell. PTHrP values for each well were normalized to the total protein content of the cell layer within the well. The *vector control line*, transduced with empty lentiviral vector, expressed negligible levels of each domain. Amino PTHrP was increased compared to vector only in the PTHrP 1–87 and PTHrP 1–139 groups, as expected. Similarly, carboxyl PTHrP increased only in the PTHrP 1–139 and PTHrP 33–139 groups. Twenty-four hour secretion of PTHrP exceeded the quantity detected in the cells by a large margin for both domains. Data represent triplicate measurements ± standard error of the mean
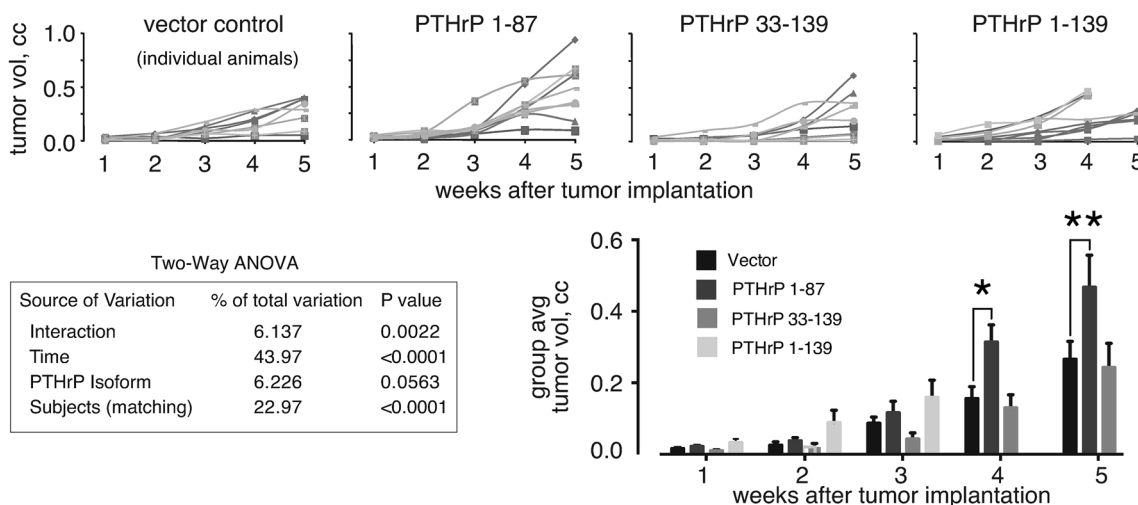
Fig. 3 Time course of tumor growth for each PTHrP isoform group. The upper row of graphs shows tumor volume (estimated from caliper dimensions) plotted versus time for individual mice in each of the groups. *Line segments* connect the tumor volumes for each individual mouse from 1 week to the next. The greatest tumor volumes were observed for mice in the PTHrP 1–87 group. On average (*lower graph*), the PTHrP 1–87 group had significantly higher volumes than did the vector control group at week 4 ($P < 0.05$) and week 5 ($P < 0.01$). Three mice in the PTHrP 1–139 group died by week 4

in that group had been euthanized by week 4. Thus, the weeks 4 and 5 data represented only the animals with the slower growing tumors. In the endpoint analysis, tumors in the PTHrP 1–87 group had almost twice the number of mitotic bodies as tumors in the vector control ($P < 0.001$) and tumors in the PTHrP 33–139 group (Fig. 4). The CD31 staining index (staining area per high-power field) was roughly seven times greater in the PTHrP 1–87 group than in the vector control group and over twice the magnitude of the staining in the PTHrP 33–139 group.

Mitotic bodies and CD31 index were not significantly increased in the PTHrP 1–139 group. Mouse weight increased for all four groups for the first 3 weeks after tumor implantation, but slowed for the PTHrP 1–87 and PTHrP 1–139 tumor groups compared to the other groups in subsequent weeks (Fig. 5). At week 5, animal weights for mice in the PTHrP 1–87 group and the PTHrP 1–139 group were lower than weights in the other groups. The PTHrP 1–87 group average weight differed significantly from the control group at week 5 ($P < 0.05$).
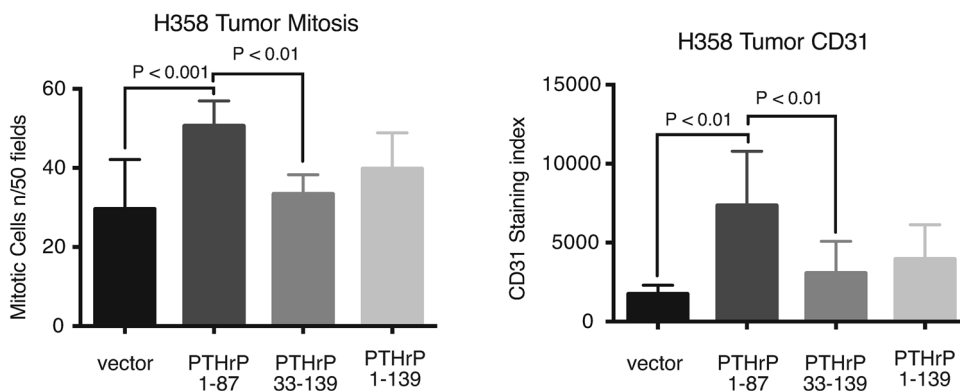
Fig. 4 Effect of PTHrP isoform on lung tumor proliferation and angiogenesis markers. *Graphs* show counts of tumor mitotic bodies/50 high-power fields (*left panel*) and a staining index, % of area with marker immunofluorescence, for CD31, an endothelial marker, for mice bearing control tumors with low PTHrP ($n=6$), and tumors overexpressing PTHrP 1–87 ($n=9$), PTHrP 33–139 ($n=7$), and PTHrP 1–139 ($n=6$). PTHrP 1–87 expressing tumors had higher numbers of mitotic bodies than control tumors ($P=0.001$), PTHrP 33–139-positive tumors ($P=0.001$), and PTHrP 1–139-positive tumors ($P=0.109$, non-significant). PTHrP 1–87 expressing tumors also had a greater CD31 staining index than control tumors ($P=0.001$), PTHrP 33–139-positive tumors ($P=0.001$), and PTHrP 1–139-positive tumors ($P=0.065$, non-significant)
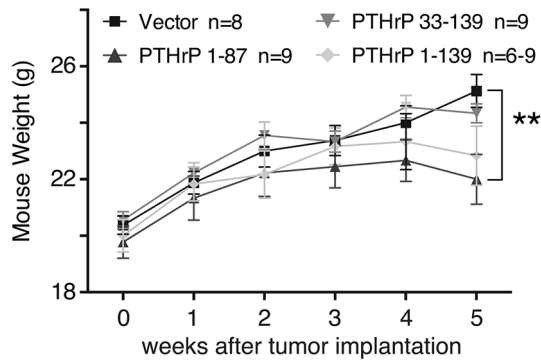
Fig. 5 Mouse weights over time based on tumor PTHrP expression. Mouse weight increased progressively with time over the 5 week after tumor implantation for the vector control mice. Growth slowed after 3 week for the PTHrP 1–87 and PTHrP 1–139 mice, and weights were 2–3 g less at week 4 and week 5 for mice in those groups on average than for mice in the control group ($P < 0.01$ for vector versus PTHrP 1–87 group)

Discussion

The first goal of this study was to reconsider the results of two previous papers, one indicating that carboxyl PTHrP was a positive prognostic indicator for survival in female patients with NSCLC (Hastings et al. 2006) and the other reporting that amino PTHrP was a negative survival factor in lung adenocarcinoma (Monego et al. 2009). Our premise was that both results could be valid because full-length PTHrP can be processed into smaller entities containing either the amino or the carboxyl PTHrP domain alone. In fact, 30–40% of the NSCLC tumors we evaluated expressed only one PTHrP domain. The TMA study then tested the survival implications of both amino PTHrP and carboxyl PTHrP. The multivariate analysis found that amino PTHrP was a significant predictor of mortality with hazard ratios of 2.0 for overall mortality ($P = 0.031$) and 2.6 for cancer-specific mortality ($P = 0.008$). Carboxyl PTHrP had hazard ratios less than 1 for overall and cancer-specific mortality, but neither case reached statistical significance ($P = 0.061$ and $P = 0.092$). Similar conclusions were drawn from a Cox analysis that counted any PTHrP immunoreactivity as a positive result, as we had done in our earlier publications regarding carboxyl PTHrP (Hastings et al. 2006). Thus, the TMA study supported previous findings by Monego and colleagues that tumor staining for amino PTHrP was associated with an increased risk of mortality in lung adenocarcinoma.

Our previous study on tumor specimens from UC San Diego (Hastings et al. 2006), as well as a confirmatory second publication (Montgrain et al. 2011) had identified carboxyl PTHrP as a positive prognostic indicator in NSCLC. Here we have conducted a post hoc assessment of amino PTHrP in a large subset of those tumors. The multivariate

hazard ratio for amino PTHrP was 1.32, missing the threshold for significance by a small margin at $P = 0.051$. Carboxyl PTHrP remained a positive prognostic indicator with a hazard ratio of 0.65 ($P = 0.003$). Thus, amino PTHrP appears as a survival factor for NSCLC in some studies, the Monego article (Monego et al. 2009) and our TMA study, while carboxyl PTHrP is the predominant survival marker in our two previous studies (Hastings et al. 2006; Montgrain et al. 2011). The relationship between tissue PTHrP staining and lung cancer patient survival may change with the patient population or the study conditions. Findings may be affected by patient demographics, including gender, cancer histology and other characteristics, covariate risk factors, and the methods used for specimen preparation and staining.

The cell culture and mouse xenograft platforms enabled controlled expression of specific PTHrP forms under reproducible experimental conditions. In cell culture, overexpression of all three PTHrP forms reduced H358 cell proliferation measured by MTS compared to cells that expressed little of either PTHrP domain. This result is consistent with the outcome of PTHrP 1–87 overexpression in H1944 lung adenocarcinoma cells from previous studies (Hastings et al. 2009; Montgrain et al. 2015). In H1944 cells, PTHrP 1–87 activated a protein kinase A-dependent process, increased expression of p27(Kip1), and decreased activity of cyclin-dependent kinase-2. Mid-molecule PTHrP and carboxyl PTHrP-terminal PTHrP have demonstrated inhibitory effects on cell growth elsewhere. For example, PTHrP 67–86, PTHrP 38–94, and PTHrP 107–139 are anti-mitogenic in breast cancer cells (Luparello et al. 1997, 1995, 2001). All of these peptides are contained within PTHrP 33–139 and PTHrP 1–139 and could have been the active inhibiting agents in H358 cells expressing those PTHrP forms in our experiments. One would not be surprised to find that mid-molecule and carboxyl PTHrP had similar effects to amino PTHrP. All three domains stimulate second messengers that are consistent with action through a G protein-coupled receptor (Orloff et al. 1994, 1996; Whitfield et al. 1994).

Xenografts formed with PTHrP 1–87 overexpressing H358 cells demonstrated significantly faster growth than did tumors formed with vector-transfected cells. The density of mitotic bodies was greater in PTHrP 1–87 overexpressing tumors than in controls, suggesting increased cell proliferation, and the CD31 staining index was also increased, suggesting increased angiogenesis compared to control tumors. Increased tumor growth in the PTHrP 1–87 group is paradoxical since PTHrP 1–87 expression inhibited H358 cell proliferation in cell culture. Amino PTHrP generated by the H358 cell xenografts could conceivably interact with the tumor microenvironment to stimulate tumor progression and dominate over any autocrine effect

of amino PTHrP on H358 cell proliferation. In contrast to PTHrP 1–87, PTHrP 1–139, and PTHrP 33–139 over-expression did not significantly augment tumor growth, mitotic bodies, or CD31 staining compared to the control group with no PTHrP overexpression.

The absence of a stimulatory effect of PTHrP 1–139 on tumor growth was unexpected. This full-length iso-form includes the amino PTHrP sequence recognized by the PTHrP receptor and other investigators have found that PTHrP 1–139 has an ability similar to that of PTHrP 1–34 to stimulate cAMP in primary vascular smooth muscle cells and UMR106 osteoblast cells (Wu et al. 1993). In our study, mice in the PTHrP 1–87 group and the PTHrP 1–139 group displayed similarly decreased weight compared to the control group and the PTHrP 33–139 group toward the end of the 5 week period (Fig. 5), an effect we attribute to the propensity of amino PTHrP–PTHrP receptor interactions to promote cachexia (Kir et al. 2014, 2016). Thus, the weight data provide circumstantial evidence for increased amino PTHrP receptor activation in both the PTHrP 1–87 and the PTHrP 1–139 groups.

The action of carboxyl PTHrP domains that are not present in PTHrP 1–87 could provide an alternative explanation for the lack of tumor growth acceleration in the PTHrP 1–139 group. An anti-mitogenic autocrine effect of car-boxyl PTHrP on H358 cell proliferation, as suggested by the cell culture MTS experiments, might balance a stimula-tory effect of amino PTHrP mediated through tumor micro-environment, but we have no evidence supporting that mechanism at this time. It does appear that the presence of carboxyl PTHrP opposes the pro-malignant action of amino PTHrP in H358 cell lung cancer xenografts.

In summary, this investigation supports an association between lung carcinoma amino PTHrP expression and an increased risk of death, as first observed by Monego and colleagues (Monego et al. 2009). In mouse studies, amino PTHrP stimulated lung carcinoma xenograft growth, con-sistent with the human studies, but the presence of carboxyl PTHrP in the xenografts reversed the growth effect. In fact, previous human studies have found a decreased risk of death in association with carboxyl PTHrP expression (Hast-ings et al. 2006; Montgrain et al. 2011). Thus, the impact of PTHrP expression on lung cancer growth and survival may depend on epitope expression and other contextual factors.

Compliance with ethical standards

Ethical approval All procedures performed in studies involving human participants were in accordance with the ethical standards of the institution research committee and with the 1964 Helsinki decla-ration and its later amendments. The local institution research board determined that the human study constituted a retrospective and satis-fied all criteria for studies where formal consent is not required. All applicable international, national, and institutional guidelines for the care and use of animals were followed.

Conflict of interest None.

References

Akino K, Ohtsuru A, Kanda K, Yasuda A, Yamamoto T, Akino Y, Naito S, Kurokawa M, Iwahori N, Yamashita S (2000) Parathy-roid hormone-related peptide is a potent tumor angiogenic factor. Endocrinology 141:4313–4316. doi:10.1210/endo.141.11.7875

Asa SL, Henderson J, Goltzman D, Drucker DJ (1990) Parathyroid hormone-like peptide in normal and neoplastic human endocrine tissues. J Clin Endocrinol Metab 71:1112–1118. doi:10.1210/jcem-71-5-1112

Bakre MM, Zhu Y, Yin H, Burton DW, Terkeltaub R, Deftos LJ, Var-ner JA (2002) Parathyroid hormone-related peptide is a naturally occurring, protein kinase A-dependent angiogenesis inhibitor. Nat Med 8:995–1003. doi:10.1038/nm753

Brandt DW, Burton DW, Gazdar AF, Oie HE, Deftos LJ (1991) All major lung cancer cell types produce parathyroid hormone-like protein: Heterogeneity assessed by high performance liquid chromatography. Endocrinology 129:2466–2470. doi:10.1210/endo-129-5-2466

Chen HL, Demiralp B, Schneider A, Koh AJ, Silve C, Wang CY, McCauley LK (2002) Parathyroid hormone and parathyroid hormone-related protein exert both pro- and anti-apoptotic effects in mesenchymal cells. J Biol Chem 277:19374–19381. doi:10.1074/jbc.M108913200

Deftos LJ (2001) Immunoassays for PTH and PTHrP. In: Bilezikian J P, Marcus R, Levine A (eds) The Parathyroids. Academic Press, San Diego, pp 143–165

Deftos LJ, Burton DW, Brandt DW (1993) Parathyroid hormone-like protein is a secretory product of atrial myocytes. J Clin Invest 92:727–735

Hastings RH, Laux AM, Casillas A, Xu R, Lukas Z, Ernstrom K, Deftos LJ (2006) Sex-specific survival advantage with PTHrP in non-small cell lung carcinoma patients. Clin Cancer Res 12:499–506. doi:10.1158/1078-0432.CCR-05-0930

Hastings RH, Montgrain PR, Quintana R, Rascon Y, Deftos LJ, Healy E (2009) Cell cycle actions of parathyroid hormone-related pro-tein in non-small cell lung carcinoma. Am J Physiol Lung Cell Mol Physiol 297:L578–L585. doi:10.1152/ajplung.90560.2008

Hirsch FR, Varella-Gardcia M, Bunn PA, Di Maria MV, Veve R, Bremmes RM, Baron ME, Zeng C, Franklin WA (2003) Epi-dermal growth factor receptor in non-small-cell lung carcino-mas: correlation between gene copy number and protein expres-sion and impact on prognosis. J Clin Oncol 21:3798–3807. doi:10.1200/JCO.2003.11.069

Hook VY, Burton D, Yasothornsrikul S, Hastings RH, Deftos LJ (2001) Proteolysis of ProPTHrP(1–141) by "prohormone thiol protease" at multibasic residues generates PTHrP-related peptides: implications for PTHrP peptide production in lung cancer cells. Biochem Biophys Res Commun 285:932–938. doi:10.1006/bbrc.2001.5249

Isowa S, Shimo T, Ibaragi S, Kurio N, Okui T, Matsubara K, Hassan NM, Kishimoto K, Sasaki A (2010) PTHrP regulates angiogen-esis and bone resorption via VEGF expression. Anticancer Res 30:2755–2767

Kir S, White JP, Kleiner S, Kazk L, Cohen P, Baracos VE, Spiegelman BM (2014) Tumour-derived PTH-related protein triggers adipose tissue browning and cancer cachexia. Nature 513:100–104. doi:10.1038/nature13528

Kir S, Komaba H, Garcia AP, Economopoulos KP, Liu W, Lanske B, Hodin RA, Spiegelman BM (2016) PTH/PTHrP receptor mediates cachexia in models of kidney failure and cancer. Cell Metab 23:315–323. doi:10.1016/j.cmet.2015.11.003

Kitazawa S, Fukase M, Kitazawa R, Takenaka A, Gotoh A, Fujita T, Maeda S (1991) Immunohistologic evaluation of parathyroid hormone-related protein in human lung cancer and normal tissue with newly developed monoclonal antibody. Cancer 67:984–989

Lee HJ, Xu X, Choe G, Chung DH, Seo JW, Lee JH, Lee CT, Jheon S, Sung SW, Chung JH (2010) Protein overexpression and gene amplification of epidermal growth factor receptor in nonsmall cell lung carcinomas: comparison of four commercially available antibodies by immunohistochemistry and fluorescence in situ hybridization study. Lung Cancer 68:375–382. doi:10.1016/j.lungcan.2009.07.014

Luparello C, Burtis WJ, Raue F, Birch MA, Gallagher JA (1995) Parathyroid hormone-related peptide and 8701-BC breast cancer cell growth and invasion in vitro: Evidence for growth-inhibiting and invasion-promoting effects. Mol Cell Endocrinol 111:225–232

Luparello C, Birch MA, Gallagher JA, Burtis WJ (1997) Clonal heterogeneity of the growth and invasive response of a human breast carcinoma cell line to parathyroid hormone-related peptide fragments. Carcinogenesis 18:23–29

Luparello C, Romanotto R, Tipa A, Sirchia R, Olmo N, Lopez de Silanes I, Turnay J, Lizarbe MA, Stewart AF (2001) Midregion parathyroid hormone-related protein inhibits growth and invasion in vitro and tumorigenesis in vivo of human breast cancer cells. J Bone Mineral Res 16:2173–2181. doi:10.1359/jbmr.2001.16.12.2173

McLemore TL, Liu MC, Blacker PC, Gregg M, Alley MC, Abbott BJ, Shoemaker RH, Bohlman ME, Litterst CC, Hubbard WC, Brennan RH, McMahon JB, Fine DL, Eggleston JC, Mayo JG, Boyd MR (1987) Novel intrapulmonary model for orthotopic propagation of human lung cancers in athymic nude mice. Cancer Res 47:5132–5140

Monego G, Lauriola L, Ramella S, D'Angelillo RM, Lanza P, Granone P, Ranelletti FO (2009) Parathyroid hormone-related peptide and parathyroid hormone-related peptide receptor type 1 expression in human lung adenocarcinoma. Chest 137:898–908. doi:10.1378/chest.09-1358

Montgrain PR, Quintana RA, Burton DW, Deftos LJ, Casillas A, Rascon YM, Hastings RH (2007) Parathyroid hormone-related protein varies with sex and androgen status in non-small cell lung cancer. Cancer 110:1313–1320. doi:10.1002/cncr.22922

Montgrain PR, Deftos LJ, Arenberg D, Tipps A, Quintana R, Carskadon S, Hastings RH (2011) Prognostic implications of parathyroid hormone-related protein in males and females with non-small cell lung cancer. Clin Lung Cancer 12:197–205. doi:10.1016/j.cllc.2011.03.018

Montgrain PR, Phun J, Vander Werff R, Quintana RA, Davani AJ, Hastings RH (2015) Parathyroid-hormone-related protein signaling mechanisms in lung carcinoma growth inhibition. Springerplus 4:268. doi:10.1186/s40064-015-1017-4

Orloff JJ, Reddy D, de Papp AE, Yang KH, Soifer NE, Stewart AF (1994) Parathyroid hormone-related protein as a prohormone: posttranslational processing and receptor interactions. Endocrine Rev 15:40–60. doi:10.1210/edrv-15-1-40

Orloff JJ, Ganz MB, Nathanson MH, Moyer MS, Kats Y, Mitnick M, Behal A, Gasalla-Herraiz J, Isales CM (1996) A midregion parathyroid hormone-related peptide mobilizes cytosolic calcium and stimulates formation of inositol trisphosphate in a squamous carcinoma cell line. Endocrinology 137:5376–5385. doi:10.1210/endo.137.12.8940360

Philbrick WM, Wysolmerski JJ, Galbraith S, Holt E, Orloff JJ, Yang KH, Vasavada RC, Weir EC, Broadus AE, Stewart AF (1996) Defining the roles of parathyroid hormone-related protein in normal physiology. Physiol Rev 76:127–173

R Development Core Team (2004) R: A language and environment for statistical computing. R Foundation for Statistical Computing. http://www.R-project.org

Tsigelny I, Burton DW, Sharikov Y, Hastings RH, Deftos LJ (2005) Coherent expression chromosome cluster analysis reveals differential regulatory functions of amino-terminal and distal parathyroid hormone-related protein domains in prostate carcinoma. J Biomed Biotechnol 2005:353–363. doi:10.1155/JBB.2005.353

Whitfield JF, Isaacs RJ, Chakravarthy BR, Durkin JP, Morley P, Neugebauer W, Williams RE, Willick G, Rixon RH (1994) C-terminal fragments of parathyroid hormone-related protein, PTHrP-(107–111) and (109–139), and the N-terminal PTHrP-(1–40) fragment stimulate membrane-associated protein kinase C activity in rat spleen lymphocytes. J Cell Physiol 158:518–522. doi:10.1002/jcp.1041580317

Wu S, Pirola CJ, Green J, Yamaguchi DT, Okano K, Juppner H, Forrester JS, Fagin JA, Clemens TL (1993) Effects of N-terminal, midregion, and C-terminal parathyroid hormone-related peptides on adenosine 3′, 5′-monophosphate and cytoplasmic free calcium in rat aortic smooth muscle cells and UMR-106 osteoblast-like cells. J Biol Chem 133:2437–2444. doi:10.1210/endo.133.6.8243262

Yam PY, Li S, Wu J, Hu J, Zaia JA, Yee JK (2002) Design of HIV vectors for efficient gene delivery into human hematopoietic cells. Mol Ther 5:479–484. doi:10.1006/mthe.2002.0558

Yee JK, Miyanohara A, LaPorte P, Bouic K, Burns BC, Friedmann T (1994) A general method for the generation of high-titer, pantropic retroviral vectors: highly efficient infection of primary hepatocytes. Proc Natl Acad Sci USA 91:9564–9568